

## ICE-SHELF TOPOGRAPHY AND STRUCTURE DETERMINED USING SATELLITE-RADAR ALTIMETRY AND LANDSAT IMAGERY

by

Simon N. Stephenson

(Science Applications Research, 4400 Forbes Boulevard, Lanham, MD 20706, U.S.A.)

and

H. Jay Zwally

(Laboratory for Oceans, NASA Goddard Space Flight Center, Greenbelt, MD 20771, U.S.A.)

### ABSTRACT

The glaciological structure and dynamics of West and Shackleton Ice Shelves, East Antarctica, are qualitatively determined using a combination of satellite remote-sensing techniques. Sketch maps traced from unenhanced imagery show the ice edge, grounding lines, flow lines, and rifts. Surface-elevation profiles and contour maps from radar altimetry provide free-board elevations of the floating ice and show flow-line undulations and rumples characteristic of grounded ice. West and Shackleton Ice Shelves consist of a combination of fast-moving ice tongues from outlet glaciers and slow-moving parts constrained by islands, ice rises, and ice rumples.

### INTRODUCTION

Restraints on ice-shelf flow and spreading are typically provided by the shear forces at the sides of grounded areas and the base of areas of partial grounding (e.g. Thomas, 1973). Two ice shelves, West and Shackleton Ice Shelves,

located along the East Antarctic coast, are unusual because they are not formed in confining embayments typical of most ice shelves. West Ice Shelf, at 67°S, 85°E, extends about 100 km from the ice-sheet grounding line along about 300 km of coastline, and Shackleton Ice Shelf, at 66°S, 96°E, similarly extends about 100 km from the grounding line along about 400 km of coastline. In contrast, most of the rest of the coastline of Wilkes Land between Amery Ice Shelf and Ross Ice Shelf consists of individual ice tongues and grounded ice sheet at the seaward margin.

Both satellite-radar altimetry and high-resolution satellite imagery were previously used for mapping in the Antarctic. For example, Lucchitta and others (1984) and Swithinbank and Lucchitta (1987) showed that detailed information on surface features could be provided by satellite imagery, particularly when it is spectrally enhanced. Lucchitta and Ferguson (1986) also used imagery collected at different times to measure the velocity of rifts or large crevasses. Zwally and others (1983) used gridded and contoured satellite data to provide regional surface-elevation contours in East Antarctica. Brooks and others (1983) combined imagery and altimetry data sets to present

TABLE I. LANDSAT IMAGES USED IN THIS STUDY

Path/Row	Acquisition date	Scene id.	Sun elevation	Sun azimuth	Scene center		
			deg	deg	lat.	long.	
<i>Shackleton Ice Shelf</i>							
116-106	4 Nov 73	E-1469-01212	29	059	65°05' S	104°35' E	
116-107	4 Nov 73	E-1469-01214	28	060	66°23' S	103°09' E	
118-106	29 Nov 72	E-1129-01353	35	062	65°22' S	101°34' E	
118-107	29 Nov 72	E-1129-01360	33	063	66°37' S	99°43' E	
119-107	23 Feb 74	E-1580-01364	20	065	66°28' S	98°50' E	
123-107	27 Feb 74	E-1584-01593	19	065	66°22' S	93°09' E	
122-106	3 Dec 72	E-1133-01583	35	063	65°21' S	95°22' E	
123-106	27 Feb 74	E-1584-01591	20	064	65°02' S	94°37' E	
121-106	2 Dec 72	E-1132-01524	35	063	65°18' S	96°54' E	
120-107	1 Jan 74	E-1527-01440	33	068	66°39' S	96°56' E	
<i>West Ice Shelf</i>							
126-107	14 Nov 73	E-1479-02191	31	061	66°26' S	88°38' E	
127-108	15 Nov 73	E-1480-02251	30	060	66°44' S	85°37' E	
127-107	15 Nov 73	E-1480-02245	31	061	66°26' S	87°11' E	
128-107	27 Mar 73	E-1247-02334	10	058	66°26' S	85°42' E	
128-108	27 Mar 73	E-1247-02340	8	059	67°45' S	84°06' E	
129-108	27 Mar 73	E-1176-02390	30	069	67°40' S	82°50' E	
129-107	15 Jan	E-1176-02383	31	068	66°21' S	84°26' E	

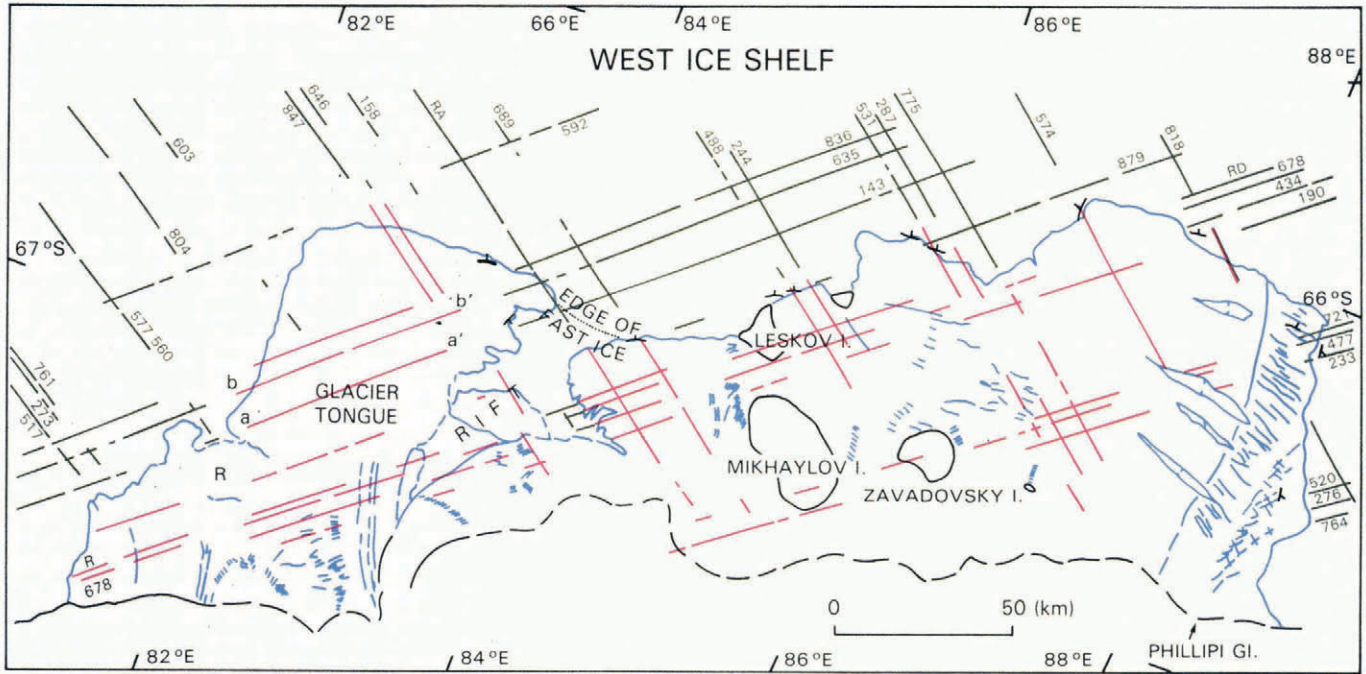


Fig. 1. Sketch map of West Ice Shelf. Black lines represent grounding lines, blue lines represent the ice-shelf margin and other boundaries within the ice shelf. Black lines also represent the ice cliffs tracked by satellite altimetry, with a tick on the side of the lower surface. Crevasses and flow bands are also shown with blue lines. The straight red and green lines are Seasat ground tracks over ice and ocean, respectively. R is an area of presumed ice rumples. Altimetry profiles for lines a-a' and b-b' are shown in Figure 6.

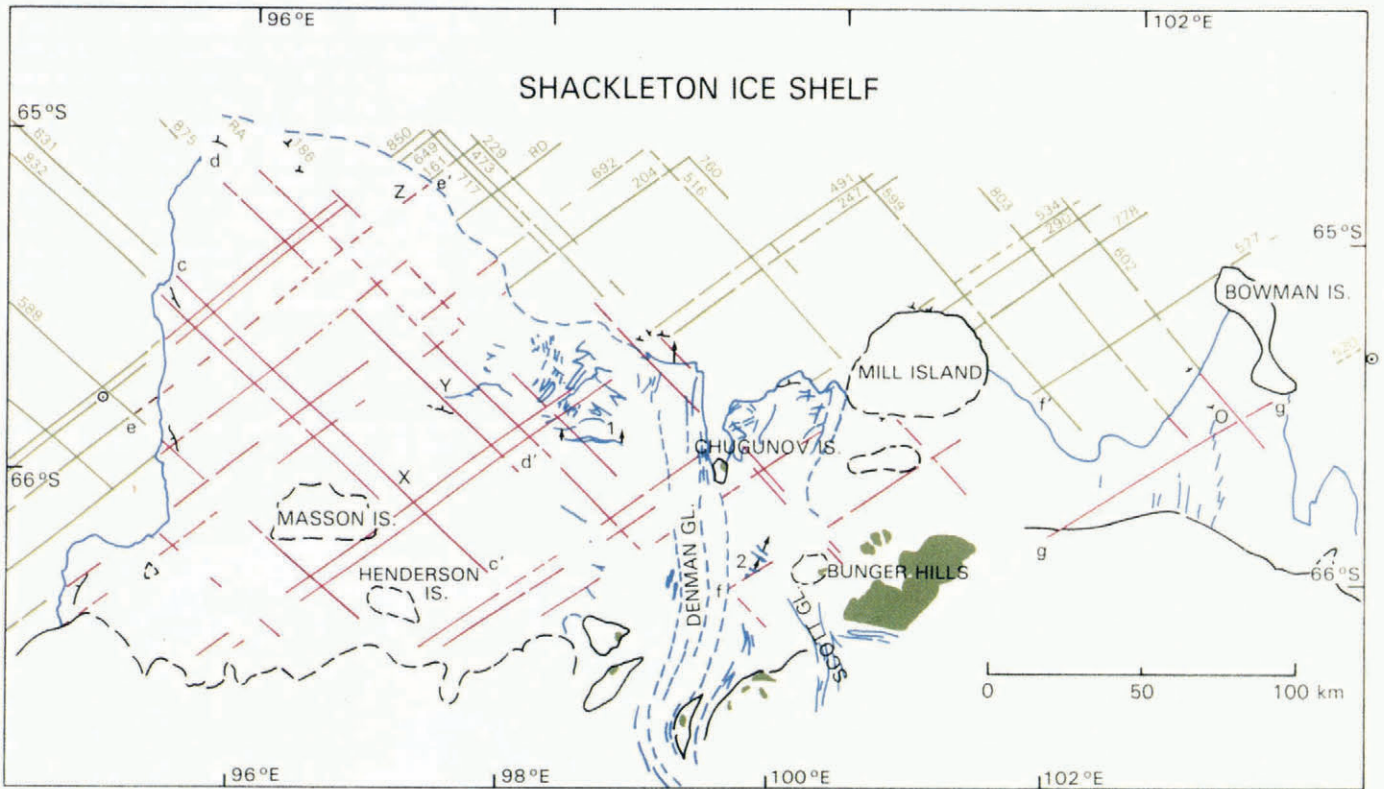


Fig. 2. Sketch map of Shackleton Ice Shelf. The symbols used are the same as those used in Figure 1, with the addition that brown areas denote rock outcrops. Altimetry profiles for lines c-c' through g-g' are shown in Figure 7.

a map of Amery Ice Shelf, and Zwally and others (1987) used radar altimetry to map ice fronts and surface elevations of Amery and Fimbul Ice Shelves.

The Landsat orbit enables imagery to be acquired north of about 82°40'S. Seasat provides elevation measurements north of 72°S, so only the coastal regions of East Antarctica and the Antarctic Peninsula are covered by both data sets. In this paper, the radar altimetry and imagery are used in combination to delineate the main features of the

glacial systems forming West and Shackleton Ice Shelves. The satellite data are confirmed by comparing the analysis with previous maps based on aerial photography and ground control.

#### SATELLITE IMAGERY

The Landsat imagery used in this analysis was obtained

from R.S. Williams of the USGS, Reston, Virginia. The imagery was acquired by Landsat-1 between November 1972 and February 1974. The scene identification numbers for the images used are given in Table I. These data are in the form of photographic prints at a scale of 1:1 000 000 on a Universal Transverse Mercator Projection. The imagery was not spectrally enhanced to optimize the identification of ice features (cf. Lucchitta and others, 1984).

The imagery, which is free of cloud cover, gives the first indication of the main glaciological units within the ice shelf. Visible features include the ice edge, some flow lines, the edges of ice rises, blue-ice zones, crevasses and rifts, and rock outcrops. Features on the images are traced, and the tracings from overlapping images are joined using rock and ice-edge features for registration. Figures 1 and 2 are the resulting line diagrams of the main glaciological features of West and Shackleton Ice Shelves, respectively. We have compared these figures with maps produced by the Australian Department of National Development (1969) and the Sovetskaya Antarkticheskaya Ekspeditsiia (Tolstikov, 1966). Some ice-shelf boundaries and rifts that were mapped by the earlier surveys are seen on the imagery recorded 30 years later. The movement of rifts and the ice edge during the 30 year interval are used to estimate ice velocities, which are discussed below.

### RADAR ALTIMETRY

The Seasat sub-satellite ground tracks, where usable data were acquired during a 3 month period ending in September 1978, are drawn in Figures 1 and 2. Although not used in this study, we note that additional data have recently been acquired by the radar altimeter on the U.S. Navy Geosat, which was launched in March 1985, also to a maximum latitude of 72°, and it is still operating at this time (Zwally and others, 1987). The gaps in the ground tracks in Figures 1 and 2 show where the Seasat radar altimeter, which was designed to track over the ocean where the surface is smooth, lost track of the signal reflected from the surface. Over irregular land and ice surfaces, the tracking algorithm was not agile enough to keep the return pulse inside the range-tracking window (Martin and others, 1983). In particular, we find that the altimeter lost track on the ice shelves at grounding lines, ice cliffs, and over crevassed or rifted regions (cf. Partington and others, 1987).

In this study, three altimeter-derived data products are

used in the analysis of ice shelves: elevation profiles, gridded and contoured surface elevations, and ice-margin maps (cf. Zwally and others, 1987). The elevation profiles are drawn from altimeter data (obtained at 10 Hz corresponding to 662 m along-track intervals), which have been corrected for deviations of the altimeter wave form from the automatic track point, for variation of atmospheric path length, and for Earth and ocean tides (Martin and others, 1983; Zwally and others, in press a). The relative accuracy of the elevations is about 1.6 m standard deviation, which includes about 1 m orbit error (Zwally and others, 1983). The elevations are plotted with respect to the GEM-10B geoid, which is within about 1 m of actual sea-level in most places. No correction is made for possible effects of radar penetration (Ridley and Partington, 1988), which are small (probably on the order of 10 cm or less) because the retracking method used (Martin and others, 1983) tends to select the range to the mean surface reflection.

Figures 3 and 4 show the contoured data of West and Shackleton Ice Shelves, respectively, with the ice fronts overlain from Figures 1 and 2. The elevation contours are produced from a gridded data set with 20 km grid spacing using an automated technique. The automated technique has some obvious limitations caused by the gridding and contouring procedure (Zwally and others, in press b) that does not accurately represent the sharp boundaries encountered in some locations and may contain other artifacts of the objective procedure. However, these contour maps reveal apparently grounded areas that might have been regarded as errors in manual contouring (see also Zwally and others, 1987), and they accurately represent the elevations in areas with sufficient data density.

The third product uses the ice-margin mapping method developed by Thomas and others (1983). The method is based on the characteristic of the altimeter that, when passing over an abrupt elevation change, it continues tracking to the original surface until the signal becomes either too noisy or too small to be detected. Zwally and others (1987) showed how this method can be used to map the ice edge of the continent as well as ice-shelf fronts. We use the same technique to map other boundaries, for example, the ice cliffs of rifts within the ice shelf. The margin-mapping technique is fairly labor intensive, but we use it here to provide better control between the Landsat imagery and the altimetry. Ice edges mapped from the altimetry data are shown in Figures 1 and 2.

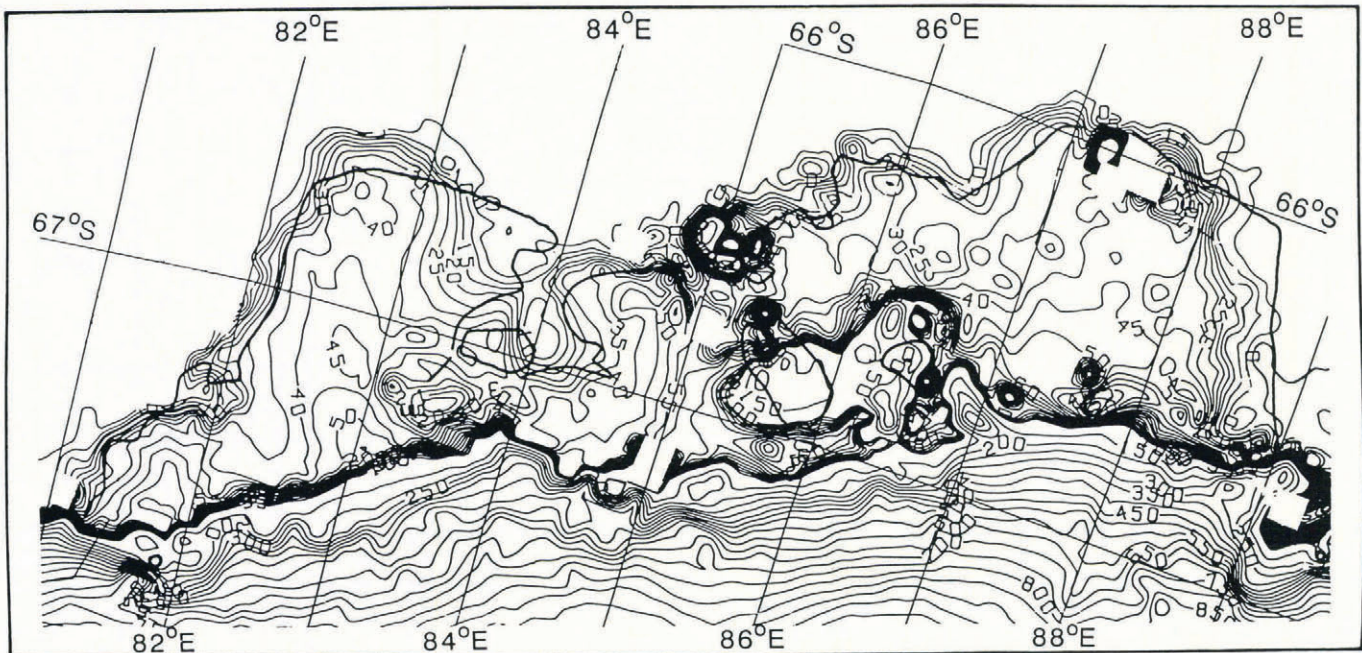


Fig. 3. Surface elevations of West Ice Shelf and adjacent grounded ice from Seasat radar altimetry compiled from a gridded data set. The thick black line represents the main features seen in Figure 1.

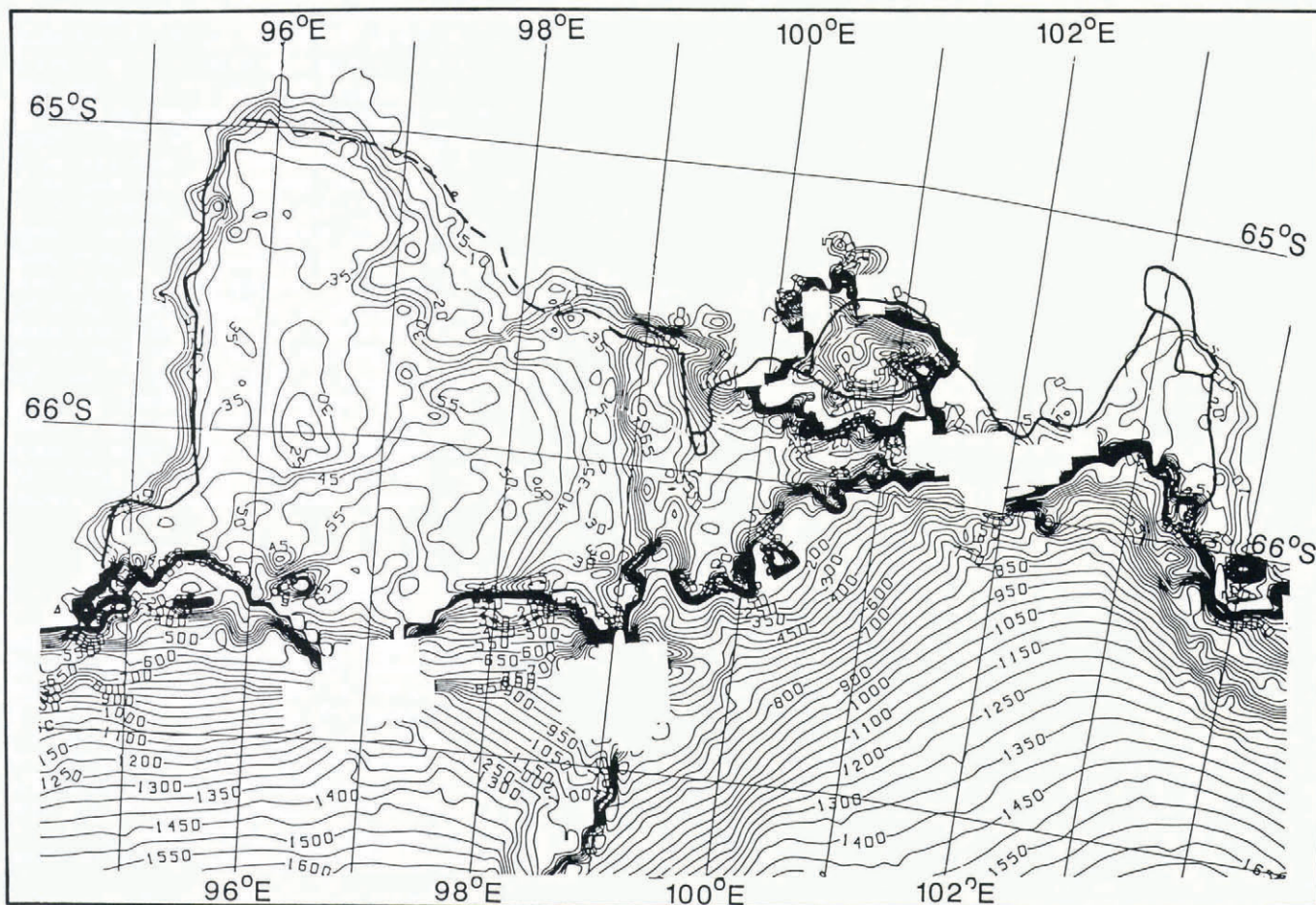


Fig. 4. Surface elevations of Shackleton Ice Shelf and adjacent grounded ice from Seasat radar altimetry compiled from a gridded data set. The thick black line represents the main features seen in Figure 2.

#### COMBINING LANDSAT DATA WITH ALTIMETRY DATA

The Landsat data are not accurately positioned geographically, and may actually be located up to 20 km from the designated scene center (personal communication from R. Ludwig). Although the authors plan to digitize the sketch maps and control them with the available ground truth, this has not been done for this study. The two data sets are spatially positioned only in local areas using edge features and ridge crests that are visible on both the altimetry and imagery. Ideally, for this purpose, the two data sets should have been acquired simultaneously. However, the Landsat data were acquired between 1972 and 1974, while the Seasat data were acquired in 1978. As a result, some of the ice margins have moved too far in the interim to be used as control features. Glacier tongues are examples of faster-moving ice, whereas the thinner parts of the ice shelves, with 10 m free-board and displacements of less than 2 km in 16 years, between 1956 and 1972, provide relatively stable ice edges. For example, such ice shelf exists between Mill and Bowman Islands on Shackleton Ice Shelf. We estimate our worst error in co-registration is about 10 km, but it is often less than 2 km.

In the unenhanced imagery used, it is often unclear what kind of ice is on either side of a boundary because it is difficult to distinguish sea ice, ice shelf, and some grounded ice. We note that, while the edges of ice rises are usually visible, ice rumpled tend to be indistinguishable from the surrounding ice shelf. The altimetry data, which are used to clarify the definition of glaciological units, also show subtle flow patterns that are not visible in the imagery because the slopes are too gradual. Once floating, the ice tends to maintain its lateral thickness gradients, although the thicker ice has been observed to expand laterally relative to the thin ice (Stephenson and Doake, 1986). Thus, the flow lines can be traced as subtle ridge

crests or troughs. In the following sections, we give examples of the features observed and discuss the dynamic implications. Where possible, we compare these observations with available ground truth from the Australian and Russian maps.

#### WEST ICE SHELF

West Ice Shelf lies between  $81^{\circ}$  and  $89^{\circ}$ E at about  $67^{\circ}$ S. Referring to Figure 1, we have labeled R a region at about  $82^{\circ}$ E to indicate a possible area of ice rumpled. The altimeter track of Rev. 879 is broken at this location, implying that the surface slope changes markedly. On the unenhanced Landsat image, the surface appears smooth but the two rifts are visible that might bound the rumpled to the north and south.

To the east of the rumpled, a large unnamed glacier tongue, about 50 km wide and extending 100 km from the grounding line, shows flow lines that are characteristic of fast glacier flow. Figure 5 shows five altimeter tracks (879, RD, 678, 434, and 190) that cross the up-stream end of the tongue where flow lines are observed on the imagery (see Fig. 1). The flow lines are indicated in the altimeter profiles of Figure 5 as small ridges, less than 10 m in height and about 5 km in width. As expected from lateral variations in the lateral strain-rates, as noted above, the ridges become less distinct further down-stream. Figure 6 shows two profiles (a-a' and b-b') across the ice tongue further down-stream. The overall curvature of the ice-tongue surface down-stream is pronounced but the small-scale flow-line ridges are more subdued than those in Figure 5.

The eastern margin of the glacier tongue is bounded by a large rift, up to 30 km wide, marking the transition between the fast ice flow in the tongue and slow flow to

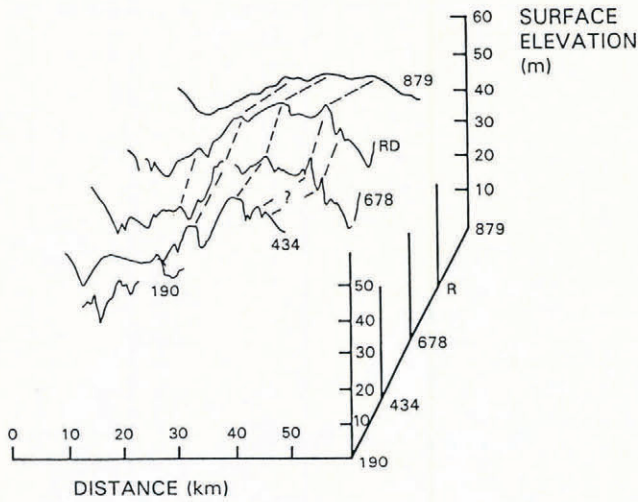


Fig. 5. Five altimetry profiles across the unnamed ice tongue that forms the west of West Ice Shelf. The peaks of undulations line up as indicated. Rev. 879 is further apart from the other revs (see Fig. 1). Gaps in the profiles are caused by the loss of an unambiguous signal.

the east. The rift does not appear on the earlier maps, although fractures up to 30 km long within the ice shelf were indicated then. The existence of the rift at the times of the earlier surveys is uncertain, because interpretation of the nature of this rift feature may have been difficult with only a few aircraft flight lines and ground observations. On the Landsat imagery, the rift is almost indistinguishable from the adjacent ice shelf. The altimeter shows that the rift contains ice, with a free-board of about 10 m, that is likely to be fast sea ice. The thickness of the sea ice would indicate either it is very old or that there has been appreciable snow accumulation. We note that there is strong katabatic redistribution of snow on the Wilkes Land coast (Goodwin, in press), which would enhance deposition within the shelter of the rifts. Sea ice of this thickness may stabilize the ice-shelf margin by decreasing the rate of calving and may also transmit shear forces between the ice tongue and the slow ice to the east. To the south of the rift there is a low piedmont-glacier area.

The slow velocity of the ice shelf between 84° and 88°E is due in part to four ice rises: Leskov, Mikhaylov, Zavadovsky, and one at the ice edge at 66°30'S, 85°40'E that was previously unmapped. There is another small ice

rise between Zavadovsky Ice Rise and the Phillippi Glacier ice tongue, which forms the eastern end of the ice shelf. The Phillippi Glacier ice tongue is 90 km in length, and is very fractured (the crevasse lines on Figure 1 are only schematic). The ice tongue appears unrestrained by grounded points but the glacier tongue and slow ice interact. Shear forces, evidenced by the presence of four large rifts up to 35 km in length west of the tongue, limit the longitudinal strain-rate of the fast ice. Also, the lateral extension of the slow ice is limited by the presence of the glacier tongue. Thus, the thinning of both is less than that of unrestrained floating ice (Weertman, 1957), allowing the ice shelf to exist for 90 km. The ice shelf forms a calving front where the free-board drops below about 30 m. The 30 m free-board height seems to be a significant factor in the formation of the calving front, as shown in Figures 3 and 4 where the 30 m contour lies just behind the ice front in many locations. The free-board at the grounding line is about 50 m. Growth of one of the rifts could cause a major calving event, but we note that the ice front varied little between the 1956 survey and the time of the Landsat imagery.

SHACKLETON ICE SHELF

The Landsat imagery covers much of Shackleton Ice Shelf except for a major section of the north-western ice shelf. The part north of 66°S, which is frequently cloud-covered, is mapped here using altimeter data only. It appears to be a smooth ice shelf (see contours in Figure 4 and profiles c-c' through e-e' in Figure 7) with an area of thinner fractured ice on the north-east margin (marked Z on Fig. 7, profile e-e'). Masson Island and the very broken ice-shelf surface north-east of the island (see Fig. 2) are at the edge of the cloud cover on the available imagery.

To the east of Henderson Ice Rise, the contoured elevations show that the flow is to the north-east towards Denman Glacier. The surface is smooth with about a 50 m free-board. The Denman Glacier ice tongue has about an 80 m free-board. Scott Glacier to the east is about 10 m lower. Both Denman and Scott Glaciers have been studied extensively by Russian and Australian field parties. The Russian map gives velocity vectors on the ice shelf between long. 98° and 102°W. Figure 8 shows the ice edge at four times: from the Australian map in 1957, Landsat imagery in 1972, Seasat altimetry in 1978, and finally from an AVHRR image in 1987. For the period 1956-78, Table II shows the implied minimum velocity (that is assuming no calving) to be 1400 ± 90 m/a, a value which agrees with the Russian

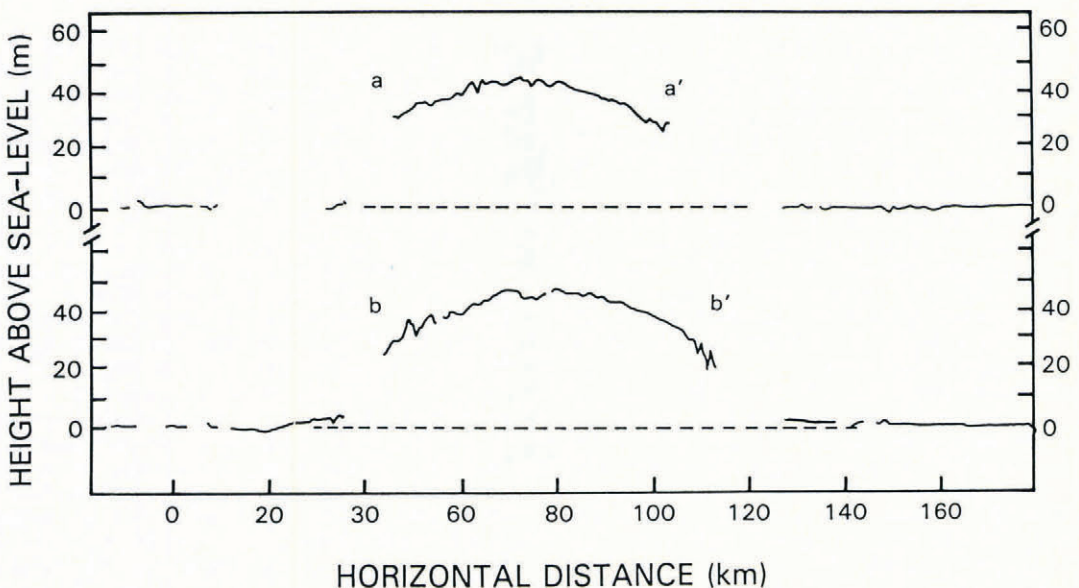


Fig. 6. Two selected surface-elevation profiles of West Ice Shelf and adjacent ocean surface plotted with respect to the measured ocean height. The positions of the profiles are shown in Figure 1. Gaps in the profile are caused by the loss of an unambiguous signal.

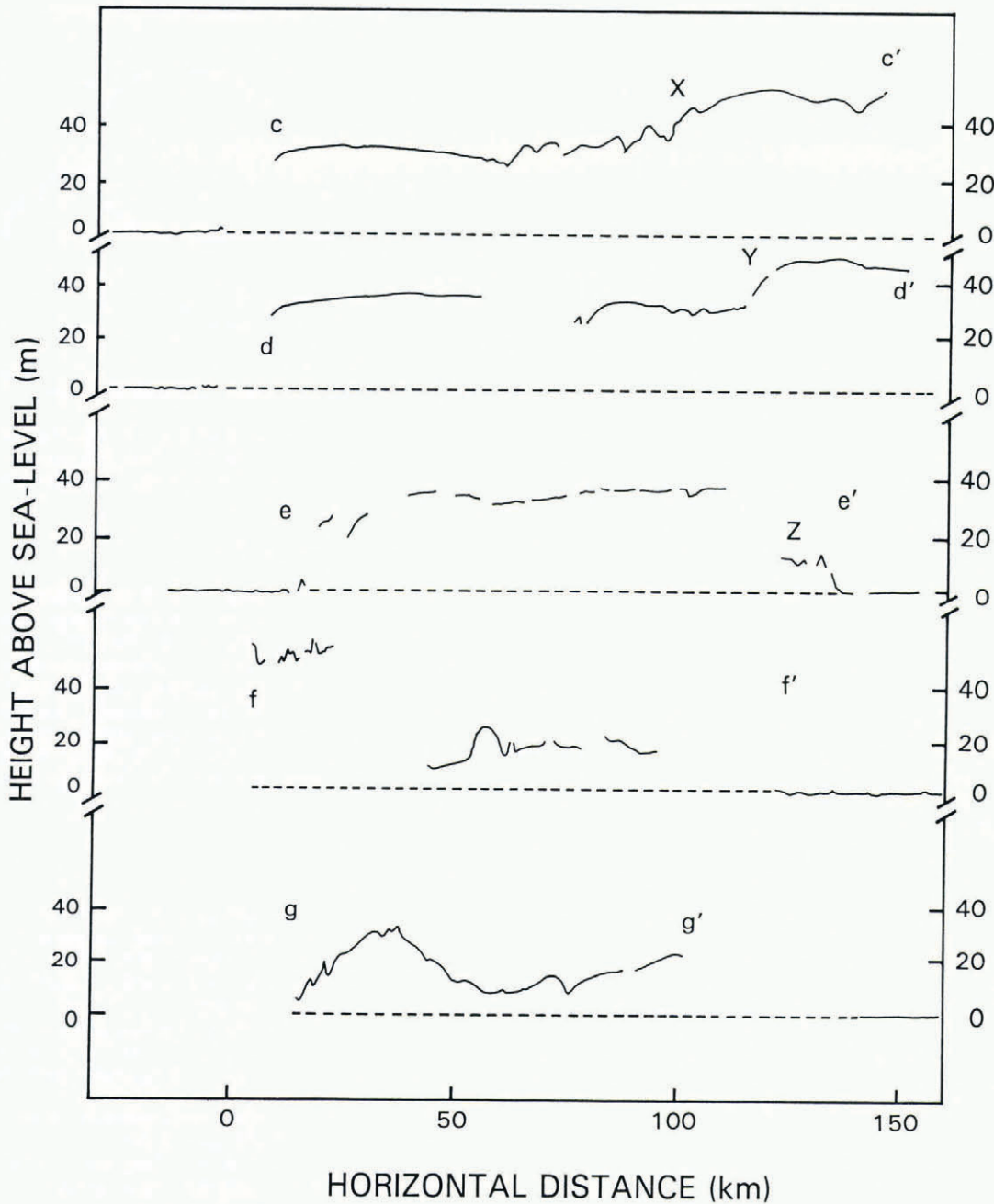


Fig. 7. Five selected surface-elevation profiles of Shackleton Ice Shelf and adjacent ocean surface plotted with respect to the measured ocean height. The positions of the profiles are shown in Figure 2. Gaps in the profile are caused by the loss of an unambiguous signal.

measurement (1452 m/a) within the limits of error. The AVHRR data of 1987 show that the ice shelf has calved back to beyond the 1957 position. Zakharov (1983) noted that the ice tongue has calved off several times since the first observations in 1914, and that the resulting icebergs sometimes ground on shallows about 100 km north of the current ice margin. In addition, several rifts mapped in 1957 are visible on the 1972 imagery. These rifts are labeled on Figure 2 and their velocities are included in Table II.

Between Mill Island and the Bunger Hills, there is only one altimetry profile (see Fig. 7, profile f-f'). The profile does not cross the unnamed ice rise south of Mill Island mapped in this area (see Fig. 2), but it shows that the ice shelf only has about 30 m free-board in this area. Because flow features are not visible, we believe that this ice is moving slowly and the ice front appears stable. Further east, the ice shelf is thinner still, with about a 10 m free-board and may have originally formed of sea ice. The ice front there also appears stable, changing little between 1957 and 1987. Small outcrops, part of the Highjump Archipelago, hold the ice front in its current position. The velocity may

be only a few meters per year. The eastern edge of the ice shelf is formed by Bowman Island.

Because there is no imagery, the dynamics of the north-western part of Shackleton Ice Shelf are more difficult to resolve. There is a significant step in the surface profiles at points marked X and Y in Figure 7 on profiles c-c' and d-d', respectively. As noted above, the contoured gridded data (Fig. 4) indicate that the flow direction is to the north-east, south-east of the X-Y line. We speculate that the ice shelf is restrained from spreading northward by ice rumpled and from spreading eastward by Denman Glacier, so it flows over ice rumpled to the north-west, thinning from a free-board of 50 m to 30 m north-west of the rumpled. The altimeter shows a rough surface for about 30 km north-west of the X-Y line and then a smooth surface, increasing gradually in height, to within 20 km of the ice edge. The higher ice might be caused by either grounding of the ice shelf on the sea bed or it might be a remnant of a period of faster ice discharge. Our preference is to speculate the existence of ice rumpled near the northern ice margin. Comparison of the AVHRR data from 1987 with the Landsat-mapped edge

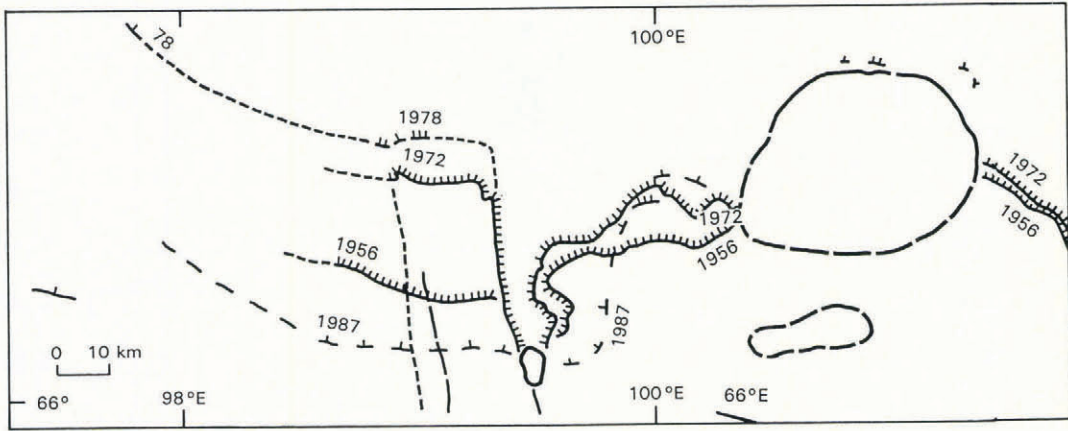


Fig. 8. Enlargement of Figure 2, showing the superposition of ice-front positions of the Denman Glacier ice tongue at four different times. The 1956 data were from Australian aerial photography, the 1972 position was from Landsat imagery, the 1978 data were derived from radar altimetry, and the 1987 data were from an AVHRR image with 4 km resolution.

shows no detectable change in the shape and position of the ice margin. If the ice shelf were unrestrained near the margin, we would anticipate measurable displacement.

CONCLUSION

Satellite-radar altimetry and high-resolution imagery in combination delineate features on the ice shelf indicative of the dynamic conditions. Qualitatively, it appears that the ice shelves are relatively stable despite the lack of embayments, because the strain-rates are restrained by islands, ice rises, and ice rumples. It is unlikely that West and Shackleton Ice Shelves would exist without the ice input from the fast glaciers, or that the glacier tongues would remain without the restraints of the adjacent slow-moving ice shelves. Sea ice may also play a stabilizing role, restraining calving within the rifts and acting as a cement for fractured ice.

Some less-stable sections of the ice shelves can be identified. It is not clear what, if anything, is restraining the north-western section of Shackleton Ice Shelf, although altimetry data suggest the possible presence of ice rumples on the north-western margin. Also, the large glacier tongue on the west end of West Ice Shelf seems unrestrained along its seaward edge, and is now only weakly coupled to the surrounding ice shelf. In either case, a major calving event could result in a new calving ice front forming at the ice rumples located 60-80 km behind the present ice edge.

Improvement in this type of analysis would follow the use of digital satellite imagery. In the future, we envisage that digitized versions of the sketch maps and altimetry data from Seasat and Geosat can be the base for quantitative modeling studies. Ice thicknesses can be derived from the free-board heights after making approximations for the ice-density profile, and ice velocities can be derived from sequential images. These data along with the ice-shelf boundaries from satellite data may be input to a model of the ice shelves such as derived by MacAyeal and Thomas (1982) in order to make a quantitative assessment of the ice shelves.

ACKNOWLEDGEMENTS

We especially thank Dr R.S. Williams again for his generous help in selecting Landsat images from the files of the U.S. Geological Survey. A. Brenner, J. Major, and H. Arabshahi of E.G. & G. Washington Analytical Services provided computer-programming and data-analysis support. N. Young and I. Goodwin provided valuable discussions based on the ground-truth data obtained by the Glaciology Section, Australian Antarctic Division. Support for this research has been provided by NASA's Oceanic Processes Program.

REFERENCES

Brooks, R.L., R.S. Williams, jr, J.G. Ferrigno, and W.B. Krabill. 1983. Amery Ice Shelf topography from satellite radar altimetry. In Oliver, R.L., P.R. James, and J.B. Jago, eds. *Antarctic earth science*. Cambridge, Cambridge University Press, 441-445.

Department of National Development. 1969. *Australian Antarctic Territory*. SQ 43-44; SQ 47-48. Canberra, Department of National Development. Division of National Mapping.

Goodwin, I. In press. Accumulation rates measured in Wilkes Land. *ANARE Res. Notes*.

Lucchitta, B.K. and H.M. Ferguson. 1986. Antarctica: measuring glacier velocity from satellite images. *Science*, 234(4780), 1105-1108.

Lucchitta, B.K., E.M. Eliason, and S. Southworth. 1984. Multispectral digital mapping of Antarctica with Landsat images. *Antarct. J. U.S.*, 19(5), 249-250.

MacAyeal, D.R. and R.H. Thomas. 1982. Numerical modeling of ice-shelf motion. *Ann. Glaciol.*, 3, 189-194.

Martin, T.V., H.J. Zwally, A.C. Brenner, and R.A. Bindschadler. 1983. Analysis and retracking of continental ice sheet radar altimeter waveforms. *J. Geophys. Res.*, 88(C3), 1608-1616.

Partington, K.C., W. Cudlip, N.F. McIntyre, and S.

TABLE II. VELOCITIES ESTIMATED FROM RIFT AND ICE-EDGE DISPLACEMENTS

Type of feature	Date of observation	Displacement	Velocity
		km	m/a
Denman Glacier ice-tongue front	1956-72	21 ± 1	1300 ± 50
Denman Glacier ice-tongue front	1972-78	9 ± 2	1500 ± 200
Rift #1 west end	1956-72	3 ± 1	180 ± 60
Rift #1 east end	1956-72	4.5 ± 1	280 ± 60
Rift #2	1956-72	3 ± 1	180 ± 60
Rift #3	1956-72	5 ± 1	310 ± 60

See Figure 2 for the location of features.

- King-Hele. 1987. Mapping of Amery Ice Shelf, Antarctica, surface features by satellite altimetry. *Ann. Glaciol.*, 9, 183-188.
- Ridley, J.K. and K.C. Partington. 1988. A model of satellite radar altimeter return from ice sheets. *Int. J. Remote Sensing*, 9(4), 601-624.
- Stephenson, S.N. and C.S.M. Doake. 1986. Strain rates on Rutford Ice Stream, Antarctica. (Abstract.) *Ann. Glaciol.*, 8, 207.
- Swithinbank, C. and B.K. Lucchitta. 1986. Multispectral digital image mapping of Antarctic ice features. *Ann. Glaciol.*, 8, 159-163.
- Thomas, R.H. 1973. The creep of ice shelves: theory. *J. Glaciol.*, 12(64), 45-53.
- Thomas, R.H., T.V. Martin, and H.J. Zwally. 1983. Mapping ice-sheet margins from radar altimetry data. *Ann. Glaciol.*, 4, 283-288.
- Tolstikov, Ye. I. ed. 1966. *Atlas Antarktiki [Antarctic atlas]*. Moskva, Glavnoye Upravleniye Geodezii i Kartografii MG SSSR.
- Weertman, J. 1957. Deformation of floating ice shelves. *J. Glaciol.*, 3(21), 38-42.
- Zakharov, V.G. 1983. Podvizhki vyvodnogo lednika Denmena i ikh svyaz' s sostoyaniyem shel'fovogo lednika Shekltona v Antarktide [Surges of the Denman outlet glacier and their relations to the state of the Shackleton Ice Shelf in Antarctica]. *Mater. Glyatsiol. Issled. Khron. Obsuzhdeniya*, 47, 75-79.
- Zwally, H.J., R.A. Bindschadler, A.C. Brenner, T.V. Martin, and R.H. Thomas. 1983. Surface elevation contours of Greenland and Antarctic ice sheets. *J. Geophys. Res.*, 88(C3), 1589-1596.
- Zwally, H.J., S.N. Stephenson, R.A. Bindschadler, and R.H. Thomas. 1987. Antarctic ice-shelf boundaries and elevations from satellite radar altimetry. *Ann. Glaciol.*, 9, 229-235.
- Zwally, H.J., R.A. Bindschadler, J.A. Major, A.C. Brenner, and T.V. Martin. In press a. *Satellite radar altimetry over ice, volume 1: processing and corrections of Seasat data over Greenland*. Greenbelt, MD, National Aeronautics and Space Administration. (NASA Tech. Memo.)
- Zwally, H.J., R.A. Bindschadler, J.A. Major, A.C. Brenner, and T.V. Martin. In press b. *Satellite radar altimetry over ice, volume 4: user's guide for Antarctic elevation data from Seasat*. Greenbelt, MD, National Aeronautics and Space Administration. (NASA Tech. Memo.)